INTERNATIONAL JOURNAL OF CLIMATOLOGY
Int. J. Climatol. **34**: 216–227 (2014)
Published online 26 February 2013 in Wiley Online Library
(wileyonlinelibrary.com) DOI: 10.1002/joc.3680

RMetS
Royal Meteorological Society

Large-scale circulation patterns favourable to tropical cyclogenesis over the western North Pacific and associated barotropic energy conversions

Tao Feng,[a,b]* Guang-Hua Chen,[b] Rong-Hui Huang[b] and Xin-Yong Shen[a]

[a] *Key Laboratory of Meteorological Disaster of Ministry of Education, Nanjing University of Information Science and Technology, Nanjing, China*

[b] *Center for Monsoon System Research, Institute of Atmospheric Physics, Chinese Academy of Sciences, Beijing, China*

ABSTRACT: Using the National Centers for Environmental Prediction-Department of Energy (NCEP-DOE) reanalysis and the Joint Typhoon Warning Center (JTWC) best track data for the period 1991–2010, this study classifies five large-scale circulation patterns in association with the tropical cyclone (TC) formation over the western North Pacific (WNP): the monsoon shear (MS), the monsoon confluence (MC), the reverse-oriented monsoon trough (RMT), the monsoon gyre (MG), and the trade wind easterlies (TE). The first three patterns account for about 80% of tropical cyclogeneses. Through a diagnosis of energetics, it is found that the tropical cyclogenesis in the MS, MC, and RMT patterns is highly associated with the barotropic energy conversion. Analysis shows that the horizontal shear of basic zonal flow provides a favourable condition for the eddy kinetic energy (EKE) growth in the MS pattern. When a TC forms in the MC pattern, the horizontal shear and convergence of basic zonal flow are both important for the EKE growth. When the basic flow is the RMT pattern, in addition to the horizontal shear of basic flow, zonal and meridional wind convergence play an important role for tropical cyclogenesis over the WNP and the South China Sea, respectively. However, the barotropic energy conversion appears not to be a main mechanism for the EKE growth in the MG and TE patterns.

KEY WORDS tropical cyclogenesis; large-scale circulation pattern; barotropic energy conversion

Received 16 May 2012; Revised 23 November 2012; Accepted 12 January 2013

1. Introduction

The influence of large-scale circulation patterns on tropical cyclogenesis over the western North Pacific (WNP) is an important issue in recent researches of typhoon climatology (Chia and Ropelewski, 2002; Lee *et al.*, 2006; Georgiadis and Bigg, 2007; Chen, 2009; Goh and Chan, 2010). Generally, a tropical cyclone (TC) forms over the tropical oceans with warm sea surface temperature (SST) (above 26.5 °C), high mid-tropospheric relative humidity, large positive low-level convergence, positive low-level relative vorticity, small vertical shear of horizontal wind (VWS) between 200 and 850 hPa (less than 5 m s^{-1}), and at a latitude enough far away from the equator (Gray, 1968). These can be considered as necessary conditions for tropical cyclogenesis (Chia and Ropelewski, 2002; Cheung, 2004).

It is known that a warm SST and oceanic mixed layer are in favour of convective activity by providing thermal energy and surface heat flux (Gray, 1998). In summer, SST in the low-latitude WNP is always above 26.5 °C (Gray, 1968). Therefore, low-level convergence, low-level vorticity, and VWS over the WNP are the most important factors controlling the TC formation (Lander, 1994; Briegel and Frank, 1997; Ritchie and Holland, 1999). Gray (1968) indicated that the TC development over the WNP is strongly controlled by the monsoon trough. Moreover, many studies showed that more than 70% of the TC geneses occur in the monsoon trough (Ritchie and Holland, 1999; Chen *et al.*, 2004).

Various large-scale circulation patterns have been identified for tropical cyclogenesis over the WNP in previous studies (Lander, 1994; Harr and Elsberry, 1995; Lander, 1996; Schreck and Molinari, 2009; Wu *et al.*, 2011). Several favourable low-level circulation patterns associated with the TC formation have been detected by Ritchie and Holland (1999). These include monsoon shear (MS) line, monsoon gyre (MG), monsoon confluence (MC) region, easterly wave, and Rossby wave energy dispersion, among which the first three patterns are related to the monsoon circulation. The MS line and MC provide a background with cyclonic shear and strong low-level convergence, and thus they can be considered as more favourable for tropical cyclogenesis than the other three patterns. Besides, upper-level trough, trade wind surges, preexisting TCs and propagating wave disturbances have

* Correspondence to: T. Feng, Center for Monsoon System Research, Institute of Atmospheric Physics, Chinese Academy of Sciences, P. O. Box 2718, Beijing 100190, China. E-mail: atao@mail.iap.ac.cn

© 2013 Royal Meteorological Society

been indicated to play significant roles in tropical cyclogenesis (Briegel and Frank, 1997; Frank and Roundy, 2006; Li and Fu, 2006; Chang *et al.*, 2010; Krouse and Sobel, 2010). Briegel and Frank (1997) proposed that an upper-level trough may interact with low-level disturbances through upper-level vorticity advection, forcing upper-level divergence and uplifting, and leading to TC formation. The trade wind surges, which are related to a mid-latitude eastward-moving high pressure system during the East Asian winter monsoon (Chang *et al.*, 2010), can strengthen the westerly winds of monsoon trough (Briegel and Frank, 1997), or easterly trade winds (Chang *et al.*, 2010). Rossby wave energy dispersion induced by a preexisting TC (Li and Fu, 2006; Fu *et al.*, 2007) could trigger another TC genesis in the cyclonic gyre of the dispersion wave train. Nevertheless, the low-level circulation is considered to be critical to the TC formation (Chen *et al.*, 2004; Ventham and Wang, 2007; Chen and Huang, 2008).

From the energy point of view, one of the most important issues is where the kinetic energy for tropical cyclogenesis comes from. The previous observational studies showed that the barotropic process in the low-troposphere over the WNP has an important influence on tropical cyclogenesis. A westward-propagating barotropic wave along the equator can accumulate the wave energy in the confluence region through the mechanism of transient energy accumulation (Webster and Chang, 1988). For example, a tropical-depression type disturbance may be seen with an approximate barotropic structure of Rossby wave, and the wave energy accumulation may be a major mechanism for the initial development of the tropical-depression type disturbance over the WNP (Sobel and Bretherton, 1999). The eastern Pacific ITCZ occasionally breaks down into multiple tropical disturbances through a process of the barotropic instability (Ferreira and Schubert, 1997). Within a monsoon trough over the WNP or a favourable low-frequency oscillation, slow-moving small-scale eddies would grow through barotropic eddy kinetic energy (EKE) conversion from the background flows, which may be favourable for tropical cyclogenesis(Maloney and Hartmann, 2001; Chen and Sui, 2010; Hsu *et al.*, 2010). Therefore, the barotropic energy conversion could be a significant source of kinetic energy for the TC formation.

Most of previous studies are focused on the environmental factors favourable to tropical cyclogenesis from statistical point of view for different large-scale patterns. However, the energy conversion in different large-scale patterns has not been addressed. The present study discusses the influences of barotropic energy conversion based on the classification of low-level circulation patterns associated with the TC formation by using 20-year data. The text is arranged as follows. Section 2 describes the dataset. Section 3 presents the definition and describes the characteristics of five low-level large-scale circulation patterns favourable to the TC genesis, and Section 4 discusses the barotropic energy conversion between eddy and flow in each large-scale pattern. Section 5 presents the conclusions and discussions.

2. Data

The TC best track dataset from the Joint Typhoon Warning Center from July to October for the period 1991–2010 is used to provide the TC information such as genesis time and location. A total number of 425 TCs during July to October are examined in this study. The warning time when the maximum sustained surface wind of a TC reaches 25 knots ($12\,m\,s^{-1}$) is defined as the genesis time. For a few cases in which tropical disturbances intensified to over 25 knots and then weakened very soon, and then re-intensified to 25 knots, the latter time is defined as the genesis time. The preformation period is defined as 72 h before the genesis time. The global atmospheric daily grid fields are from the National Centers for Environmental Prediction-Department of Energy (NCEP-DOE) AMIP-II Reanalysis (R2) with a horizontal resolution of $2.5^\circ \times 2.5^\circ$ (Kanamitsu *et al.*, 2002). The Advanced Very High Resolution Radiometer National Oceanic and Atmospheric Administration outgoing long wave radiation (OLR) product with resolution of $2.5^\circ \times 2.5^\circ$ during this period is obtained as an indication for convective activity.

3. Circulation patterns related to the TC genesis over the WNP

3.1. Classification of low-level circulation patterns related to the TC genesis

According to the feature of 850 hPa flow, the low-level circulations associated with tropical cyclogenesis over the WNP are categorized into following typical patterns: MS, MC, MG, reverse-oriented monsoon trough (RMT), trade wind easterlies (TE). The categories of wave energy dispersion and easterly waves as described by Ritchie and Holland (1999) are not included in this study. A number of cases associated with the wave energy dispersion can be classified into the MS pattern or the MC pattern due to the similarity in low-level circulation and the high correlation between the Rossby energy dispersion pattern and the MC pattern (Yoshida and Ishikawa, 2013). The RMT pattern is added in our classification because it frequently appears over the WNP. Furthermore, tropical cyclogeneses in this pattern can occur in relatively higher latitudes with different low-level barotropic dynamical process from those in lower latitudes.

An MS pattern is established when strong westerly winds and southeasterly winds coexist to the south and north of the TC genesis position during the 72-h preformation period. The MS pattern corresponds to the western part of the monsoon trough where there are large cyclonic shear and strong convergence. The TC genesis area in the MS pattern extends from the South China Sea (SCS) to the tropical central Pacific. The composite

© 2013 Royal Meteorological Society

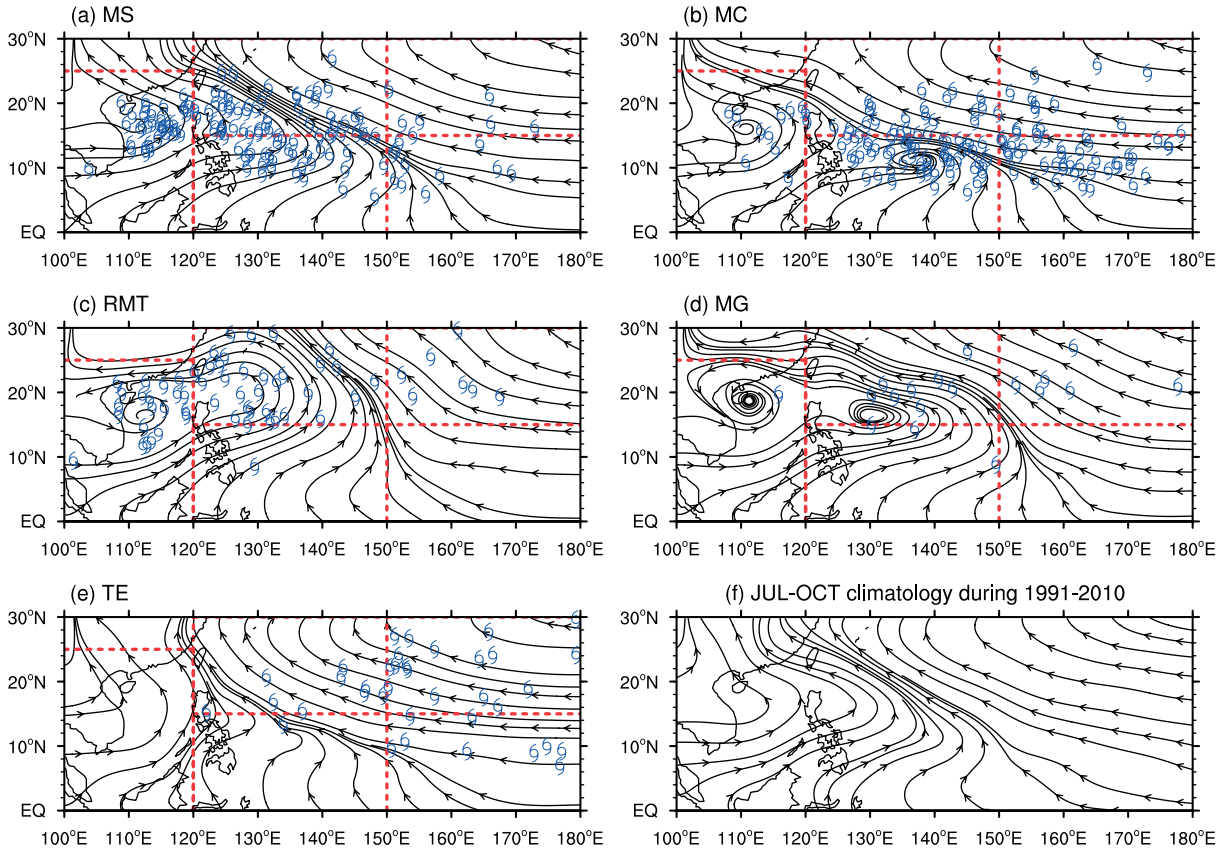

Figure 1. Composite of 850 hPa horizontal wind (Streamline) for each large-scale pattern. (a) MS pattern; (b) MC pattern; (c) RMT pattern; (d) MG pattern; (e) TE pattern; (f) July–October climatology during 1991–2010. Typhoon symbols denote the location of TCs genesis. By dash lines, the entire region is divided into five quadrants which stand for each comparable TC genesis region. Each quadrant defines as: SCS (100°E–120°E, 0°N–25°N), NW (120°E–150°E, 15°N–30°N), SW (120°E–150°E, 0°N–15°N), NE (150°E–180°E, 15°N–30°N), SE (150°E–180°E, 0°N–15°N).

Table 1. Summary of tropical cyclone cases in each large-scale pattern.

Pattern	No. (%)	SW	SE	NW	NE	SCS	Out
MS	140 (32.9)	34	13	49	6	38	0
MC	141 (33.2)	51	39	26	14	11	0
RMT	64 (15.1)	1	0	32	7	20	4
MG	18 (4.2)	3	0	8	6	1	0
TE	37 (8.7)	1	9	9	18	0	0
Other	25 (5.9)	0	0	9	8	1	7
All	425 (100)	90	61	133	59	71	11

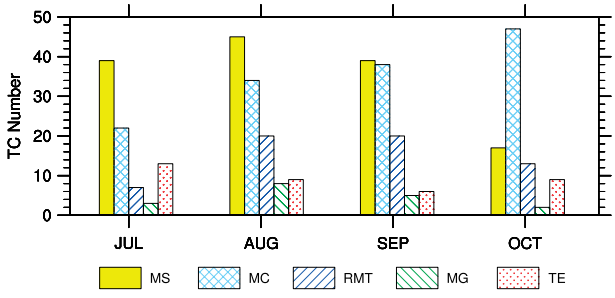

Figure 2. The monthly variation of tropical cyclogenesis events in each low-level circulation pattern during cyclone seasons in the WNP.

850 hPa flow and genesis positions in the MS pattern are shown as Figure 1(a). The composite streamline in the MS pattern is similar to the July–October climatology during 1991–2010 (Figure 1(f)).

The MC pattern is identified when there are easterly and westerly flow to the east and west of the TC genesis region, respectively, and strong southerly winds to the south are usually observed. The MC pattern represents a confluence region between westerly monsoon flow and the easterly trade winds, which is important for maintaining the moist convection and triggering a series of scale interactions. The composite 850 hPa flow in this pattern (Figure 1(b)) is different from the climatology (Figure 1(f)), that the monsoon trough break into a MS region (extend to approximate 125°E) and MC region (centred at 140°N).

In the MS pattern, the shear zone extends in the northwest-southeast orientation. On some special occasions in summer, the axis of shear line could be oriented in the southwest-northeast direction, reaching farther northward and eastward than normal. In this case, northeasterly flows are present to the north of TC genesis location, leading to unusual TC tracks (Lander, 1996). Such pattern, denoted as the RMT pattern,

© 2013 Royal Meteorological Society

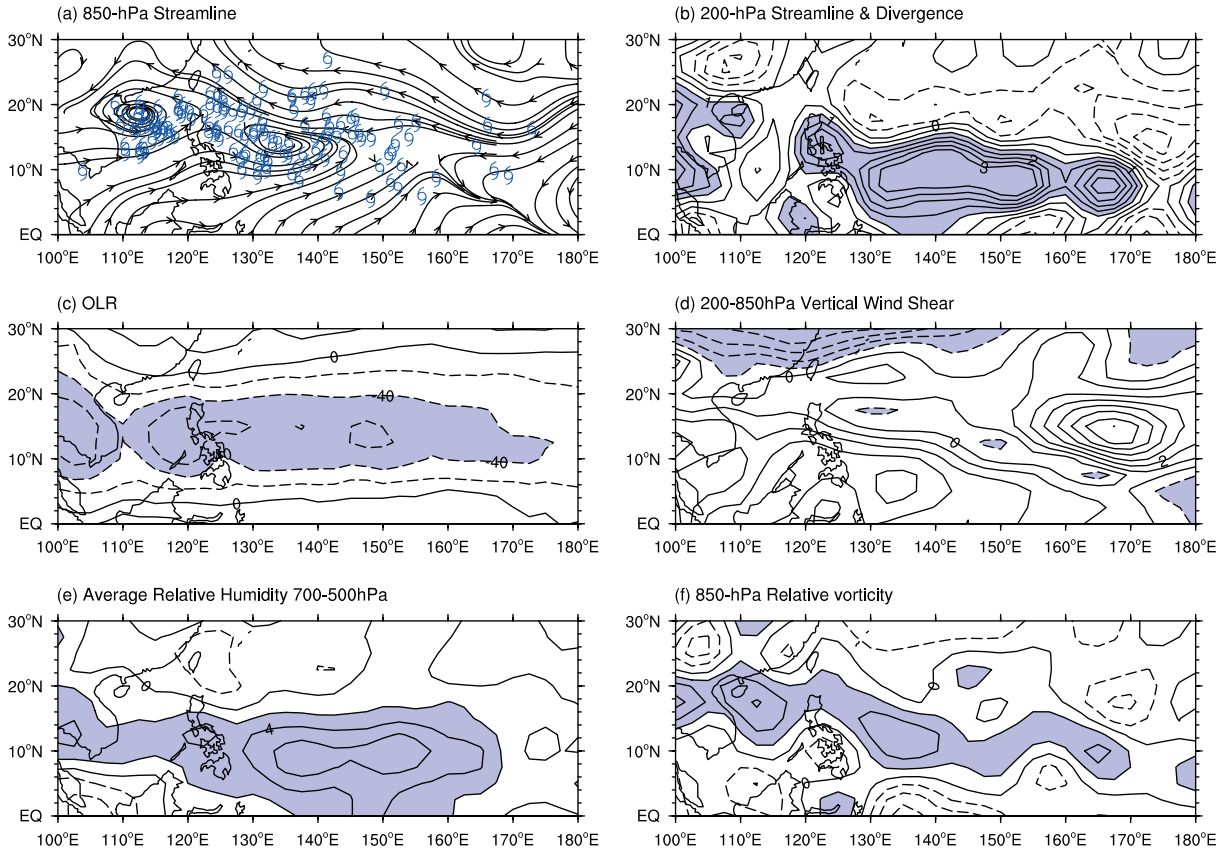

Figure 3. Composite anomaly of TC formed in the MS pattern averaged the 3-d data during pre-formation period. The 20-year climatology of each fields are subtracted from total fields. (a) 850 hPa horizontal wind (streamline) and TC genesis position (typhoon symbol); (b) 200 hPa divergence (shaded, unit: $10^{-6}s^{-1}$, contour interval is 0.5); (c) OLR ($W\,m^{-2}$), contour interval is 20; (d) 200–850 hPa vertical wind shear ($m\,s^{-1}$), contour interval is 1; (e) 700–500 hPa averaged relative humidity(%), contour interval is 2; (f) 850 hPa relative vorticity ($10^{-5}s^{-1}$), contour interval is 0.2.

features monsoon-related westerlies to the south and northeasterlies to the north with a cyclonic shear. The composite 850 hPa flow corresponding to the RMT pattern shown as Figure 1(c) is significant distinguished from the climatology (Figure 1(f)).

Lander (1994) described a characteristic large-scale circulation favourable to tropical cyclogenesis, which is named as MG. It is characterized by Lander (1994) that a cyclonic vortex with a large-scale low-level depression established usually to the northeast of the climatological position of monsoon trough with a life span of 2 or 3 weeks. The typical MG is observed on average once every 2 years in the WNP. The number of TCs that form in this special circulation is sensitive to the definition of MG. On the basis of a rather strict definition for the MG, Ritchie and Holland (1999) found that the MG pattern occurred only once within the 8 years. As a result, only 3% of all TC geneses occurred in the MG pattern. However, Chen *et al.* (2004) documented that 70% of the WNP TC geneses are linked to MGs using a looser definition for the MG. In this study, the MG pattern is defined as follows: A nearly closed vortex with diameter $\geq$ 2500km in the 850 hPa streamline chart, an isolated cyclonic vortex over the central WNP, and convection activity occurring in the southeast quadrant of the gyre vortex and lasting for 72 h prior to the TC formation. This definition is looser than that used by Ritchie and Holland (1999), but stricter than that by Chen *et al.* (2004). This ensures us to obtain enough samples and, at the same time, to maintain the dynamic features of large-scale circulation. The composite 850 hPa flow for the MG pattern is shown as Figure 1(d). On the composition map, the background flow looks like the MS pattern (Figure 1(a)) and the climatology (Figure 1(f)). This implies that the MG pattern is just another special configuration of the monsoon trough.

Though a large fraction of TCs are generated in favourable monsoon circulations as described above, a small number of TCs form in the TE flow. If the TE are prevalent around the genesis location during the 72 h prior to the TC genesis, this is denoted as the TE pattern. The composite 850 hPa flow for the TE pattern is shown as Figure 1(e).

As introduced above, the criterions for classifying each large-scale patterns are based on synoptic analysis. Because of the variety of circulation patterns, it is difficult to do rigorous classification of the low-level pattern when a TC is forming. Thus, a subjective decision is needed to select the primary patterns. Although no absolutely objective criterion is applied in this study, credible results

© 2013 Royal Meteorological Society

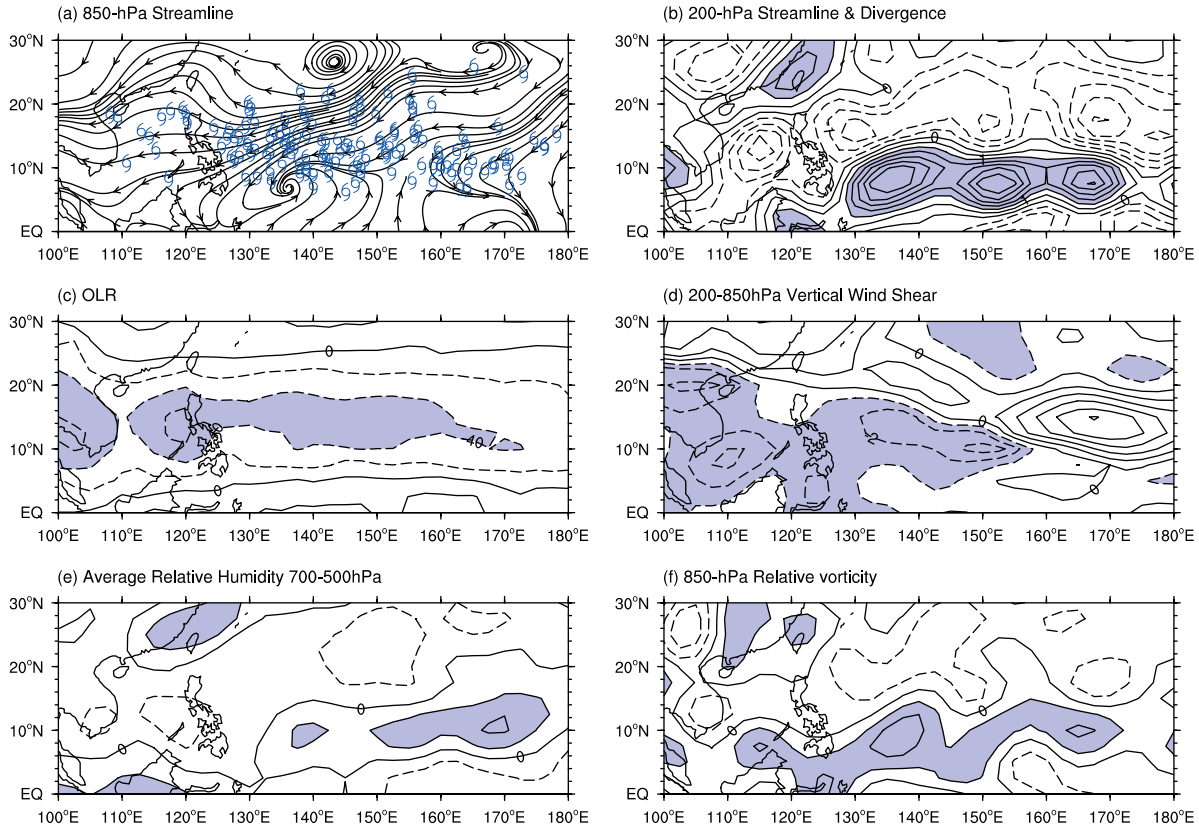

Figure 4. Composite anomaly of TC formed in the MC pattern averaged the 3-d data during pre-formation period. The 20-year climatology of each fields are subtracted from total fields. (a) 850 hPa horizontal wind (streamline) and TC genesis position (typhoon symbol); (b) 200 hPa divergence (shaded, unit: $10^{-6}s^{-1}$, contour interval is 0.5); (c) OLR ($W\,m^{-2}$), contour interval is 20; (d) 200–850 hPa vertical wind shear ($m\,s^{-1}$), contour interval is 1; (e) 700–500 hPa averaged relative humidity(%), contour interval is 2; (f) 850 hPa relative vorticity ($10^{-5}s^{-1}$), contour interval is 0.2.

were drawn after we compared our results to previous studies (Ritchie and Holland, 1999; Lee *et al.*, 2008). The results were not shown.

3.2. Differences among TC genesis in the different large-scale patterns

Table 1 presents the summary of all 425 TC genesis cases over the WNP during the typhoon season (July through October). The MS and MC patterns are the two principle patterns for the TC genesis over the WNP. The number of TC geneses in these two categories account for 32.9% and 33.2% of total events, respectively. The number of TC geneses in the RMT pattern is responsible for approximate 15.1% of all cases. The MS and RMT patterns are responsible for 48.0% of total TC geneses, which is comparable to the result of Briegel and Frank (1997), Ritchie and Holland (1999), and Lee *et al.* (2008). All monsoon-related TC geneses (MS + MC + MG + RMT) reach a percentage of 85.4%. The ratio of TC geneses in the MG pattern only account for 4.2% in spite of a loose definition, while there are only 8.7% of TC geneses in the TE pattern. In addition, 25 cases cannot be categorized into any of the above-mentioned five patterns due to their complicated circulation background. However, it is found that most of these uncategorized cases occur in higher latitude and could be attributed to the sophisticated interaction between low latitude and middle latitude systems.

There are significant differences in TC genesis locations among the five circulation patterns. For a better understanding of TC genesis location in each pattern, the WNP region is divided into five domains as shown in Figure 1. The TCs in the MS pattern are mainly generated in the SCS, northwest (NW) and southwest (SW) quadrants of the WNP (Figure 1(a)). TCs associated with the MC pattern are mainly located in the SW and southeast (SE) quadrants of the WNP (Figure 1(b)). TCs in the MG pattern usually occur in the NW and northeast (NE) quadrants of the WNP as shown in Figure 1(c), which is consistent with previous studies that the MG pattern usually occurs in higher latitude (Lander, 1994; Ritchie and Holland, 1999). Besides, TCs related to the RMT pattern tend to occur in the SCS and NW quadrant of the WNP along the main axis of the southwest-northeast orientated trough, as shown in Figure 1(d). In the TE pattern, TCs mainly occur in the NE quadrant of the WNP (Figure 1(e)).

There are obvious differences in the active period of TC genesis corresponding to these large-scale patterns. Figure 2 shows the TC number in individual months for the five large-scale patterns. Clearly, the tropical cyclogenesis associated with each pattern displays different

© 2013 Royal Meteorological Society

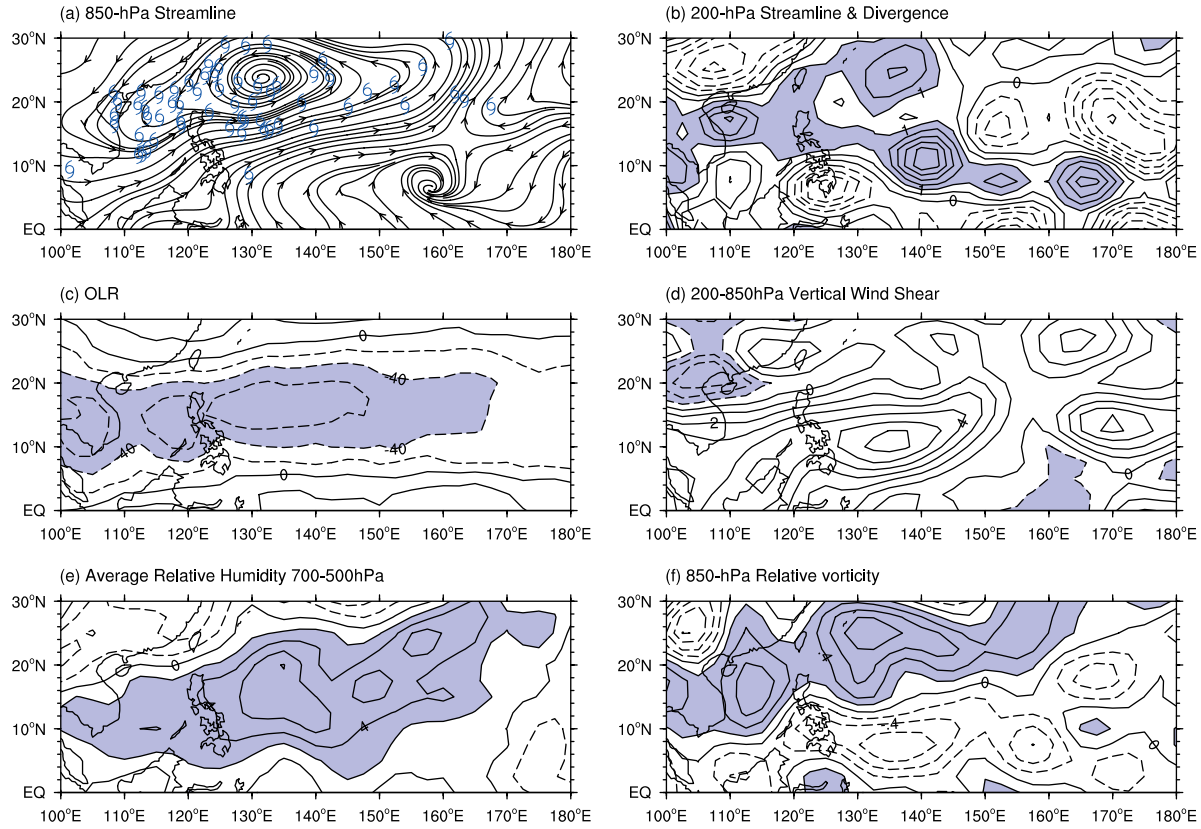

Figure 5. Composite anomaly of TC formed in the RMT pattern averaged the 3-d data during pre-formation period. The 20-year climatology of each fields are subtracted from total fields. (a) 850 hPa horizontal wind (streamline) and TC genesis position (typhoon symbol); (b) 200 hPa divergence (shaded, unit: $10^{-6}s^{-1}$, contour interval is 0.5); (c) OLR ($W\,m^{-2}$), contour interval is 20; (d) 200–850 hPa vertical wind shear ($m\,s^{-1}$), contour interval is 1; (e) 700–500 hPa averaged relative humidity(%), contour interval is 2; (f) 850 hPa relative vorticity ($10^{-5}s^{-1}$), contour interval is 0.2.

monthly variation during the typhoon season. The MS pattern related tropical cyclogeneses mostly occur from July to September when the monsoon trough is prevalent. In October, with the westward shift of the monsoon trough, the MC pattern related TC formation becomes predominant. The TCs corresponding to the RMT and MG patterns usually occur in August and September when the monsoon flow is strong. The TCs in the TE pattern are relatively frequent in July.

3.3. Main features of large-scale environment

A composite analysis is made for each large-scale pattern to examine the differences in large-scale conditions associated with tropical cyclogenesis in different categories. The composite is based on the average for the 3-day period right before the formation of TCs. The 20-year climatology is subtracted in the composite. The results are shown in Figures 3–7 for different categories.

In the MS pattern, two cyclonic vortices exist over the SCS and to the east of the Philippines, respectively (Figure 3(a)). Correspondingly, there are positive relative vorticity anomalies at 850 hPa in the above two regions (Figure 3(f)). These two areas match the main regions of TC genesis in the MS pattern. In the southern part of the main TC genesis regions, there are enhanced convection with the OLR anomalies less than $-40\,W\,s^{-2}$ (Figure 3(c)), a positive divergence anomaly region at 200 hPa extending from the Philippines to the eastern part of the WNP with an anomaly centre located over the Philippines (Figure 3(b)), and positive relative humidity in the middle troposphere (Figure 3(e)). An increase in the VWS is seen in a large part of tropical western Pacific (Figure 3(d)). Nevertheless, along the main TC genesis regions, the VWS anomaly is relatively small. Thus, it appears that in this category the TC genesis is mainly due to low-level vorticity and convergence, upper-level divergence, and mid-tropospheric humidity.

In the MC pattern, an anomalous cyclonic vortex with a centre located at 136°E, 7°N appears over the WNP (Figure 4(a)). TCs mostly form in anomalous northeasterly flow to the north of this vortex. The anomaly distribution of OLR is similar to that in the MS pattern (Figure 4(c)). The main TC genesis region is situated to the north side of positive cyclonic vorticity anomaly (Figure 4(f)), upper-level divergence anomaly (Figure 4(b)), and positive relative humidity anomaly at mid-troposphere (Figure 4(e)). These features are similar to the MS pattern. In most of the TC genesis region, the VWS anomaly is either small or negative (Figure 4(d)).

As mentioned above, the RMT pattern is characterized by a southwest-northeast oriented trough axis extending to the subtropics. This feature is clearly

© 2013 Royal Meteorological Society

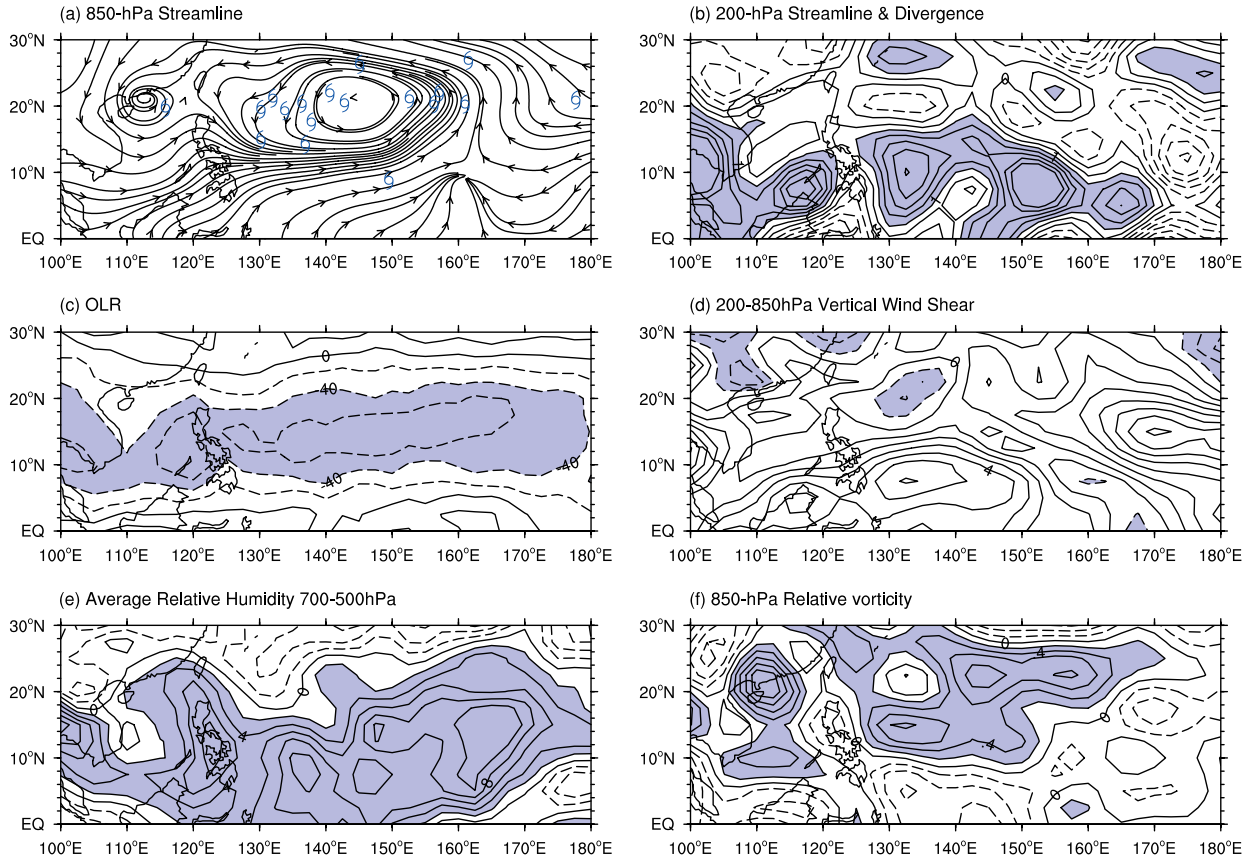

Figure 6. Composite anomaly of TC formed in the MG pattern averaged the 3-d data during pre-formation period. The 20-year climatology of each fields are subtracted from total fields. (a) 850 hPa horizontal wind (streamline) and TC genesis position (typhoon symbol); (b) 200 hPa divergence (shaded, unit: $10^{-6}s^{-1}$, contour interval is 0.5); (c) OLR ($W\,m^{-2}$), contour interval is 20; (d) 200–850 hPa vertical wind shear ($m\,s^{-1}$), contour interval is 1; (e) 700–500 hPa averaged relative humidity(%), contour interval is 2; (f) 850 hPa relative vorticity ($10^{-5}s^{-1}$), contour interval is 0.2.

seen in Figure 5(a) that shows cyclonic anomaly at 850 hPa from northern SCS to the east of Taiwan and TC geneses mostly around the anomalous vortex. This is also the region with upper-level strong divergence anomaly (Figure 5(b)), low-level positive vorticity anomaly (Figure 5(f)), and positive humidity anomaly (Figure 5(e)). In the southern part of the main TC genesis region, convection is enhanced (Figure 5(c)). In the TC genesis region, the VWS is small (Figure 5(d)). However, a large positive VWS anomaly covers a large fraction of the region to the south of 15°N, which may restrain tropical cyclogenesis in the low-latitude regions of the western Pacific Ocean.

For TCs in the MG pattern, a cyclonic circulation anomaly at 850 hPa extends over subtropical WNP (Figure 6(a)). This corresponds to positive low-level relative vorticity anomaly (Figure 6(f)). In most of the TC genesis region, the upper-level divergence anomaly is small (Figure 6(b)). Meanwhile, a negative VWS anomaly is seen in the main TC genesis region (Figure 6(d)). The mid-level troposphere is wetter than normal in tropical WNP (Figure 6(e)). Anomalously active convection is seen in the TC genesis region (Figure 6(c)). It seems that when the MG circulation forms over the WNP, a favourable dynamic and thermodynamic environment may be established for tropical cyclogenesis, as pointed out by Lander (1994).

Tropical cyclogeneses in the TE pattern prefer to occur when the Asian monsoon trough retreats westward and easterlies dominate most of the WNP (Figure 1(e)). This is clearly seen in the enhanced easterlies and the accompanying low-level convergence anomaly (Figure 7(a)). In most of the TC genesis region, convection is enhanced (Figure 7(c)) although the upper-level divergence appears to be weaker than normal (Figure 7(b)). Besides, the VWS anomaly is small in the TC genesis region except for the SE corner (Figure 7(d)). The relative vorticity and relative humidity do not show clear signal for the TC formation (Figure. 7(e) and (f)). This kind of TC genesis could be recognized as a local event.

4. The barotropic energy conversion in different large-scale circulation patterns

In this section, we examine what are the main processes in the barotropic EKE conversion between mean flow and eddy in the five large-scale circulation patterns. Following Maloney and Hartmann (2001), the barotropic kinetic energy conversion between mean flow and eddy

© 2013 Royal Meteorological Society

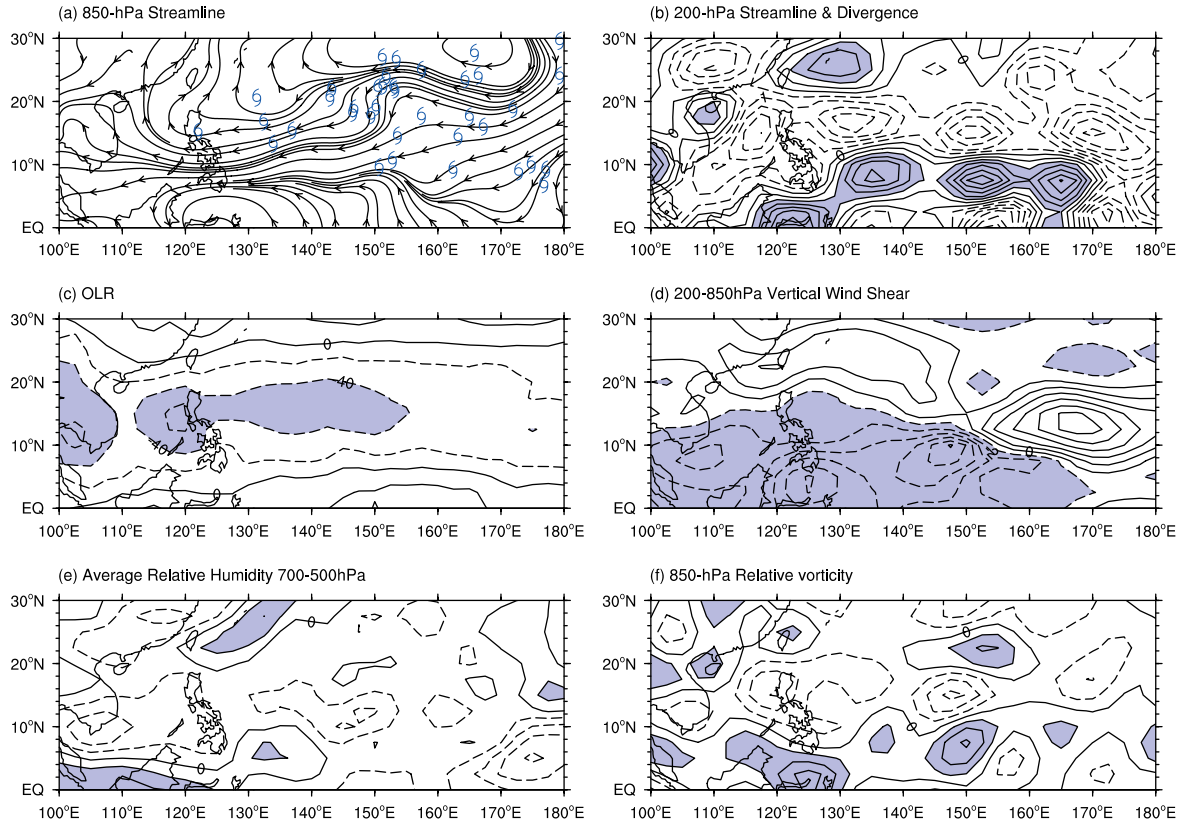

Figure 7. Composite anomaly of TC formed in the TE pattern averaged the 3-d data during pre-formation period. The 20-year climatology of each fields are subtracted from total fields. (a) 850 hPa horizontal wind (streamline) and TC genesis position (typhoon symbol); (b) 200 hPa divergence (shaded, unit: $10^{-6}s^{-1}$, contour interval is 0.5); (c) OLR ($W\,m^{-2}$), contour interval is 20; (d) 200–850 hPa vertical wind shear ($m\,s^{-1}$), contour interval is 1; (e) 700–500 hPa averaged relative humidity(%), contour interval is 2; (f) 850 hPa relative vorticity ($10^{-5}s^{-1}$), contour interval is 0.2.

is defined as follows:

$$\frac{\partial K'_{\text{baro}}}{\partial t} = -\overline{u'v'}\frac{\partial}{\partial y}\overline{u} - \overline{u'v'}\frac{\partial}{\partial x}\overline{v} - \overline{u'^2}\frac{\partial}{\partial x}\overline{u} - \overline{v'^2}\frac{\partial}{\partial y}\overline{v} \quad (1)$$

In Equation (1), (u ', v ') are the 3 to 8-d filtered winds, which represent synoptic scale disturbance as the 'seed' for tropical cyclogenesis. In view of the life span of the large-scale patterns, the mean state ($\overline{u}, \overline{v}$) is obtained by using a 10-d low-pass filter. Thus, the combined effect of intraseasonal oscillation and low-frequency background state to the EKE growth is considered in this study.

The term on the left-hand-side of Equation (1) is the tendency of barotropic energy conversion, which represents the conversion rate from mean kinetic energy to EKE. The first to the fourth term in the right side of Equation (1) indicates the contribution of the meridional shear of mean zonal winds, the zonal shear of mean meridional winds, the zonal convergence of mean zonal winds, and the meridional convergence of mean meridional winds to the increase of kinetic energy of eddy. For example, when mean zonal winds have cyclonic shear, the kinetic energy of the eddy in the mean flow will increase, i.e. the eddy may intensify. When mean zonal winds are convergent in the zonal direction, the eddy will get the kinetic energy from the mean flow and may intensify. Thus, the increase of barotropic kinetic energy of an eddy in a mean large-scale circulation pattern is closely associated with the meridional and zonal shear and convergence of the large-scale winds.

To diagnose the dynamical effect of the abovementioned large-scale circulation patterns on the TC genesis over the WNP through the barotropic energy conversion, the NCEP/NCAR reanalysis data is used to calculate the total contributions of these four terms in the right side of Equation ((1) to the increase of EKE in each large-scale circulation pattern, respectively. Figure 8 shows the composite horizontal distributions of the changing rate of EKE at 850 hPa due to the barotropic energy conversion, i.e. $\partial K'_{\text{baro}}/\partial t$, for TC genesis in the abovementioned large-scale patterns during 1991–2010. The heavy polygon boxes in Figure 8(a)–(e) are the areas where TCs form preferably. As shown in Figure 8(a)–(c), in the MS, MC, and RMT patterns, the large changing rate of EKE due to the barotropic energy conversion, i.e. $\partial K'_{\text{baro}}/\partial t$, corresponds to the main area of TC genesis. However, in the MG and TE patterns, the large values of $\partial K'_{\text{baro}}/\partial t$ do not match with the main area of TC genesis, as shown in Figure 8(d) and (e). In these two patterns, the main area of TC genesis is located to the north of the large values of $\partial K'_{\text{baro}}/\partial t$. This indicates that tropical cyclogenesis in the MG and TE patterns may not be due to the barotropic energy conversion, but may be due to other mechanism.

© 2013 Royal Meteorological Society

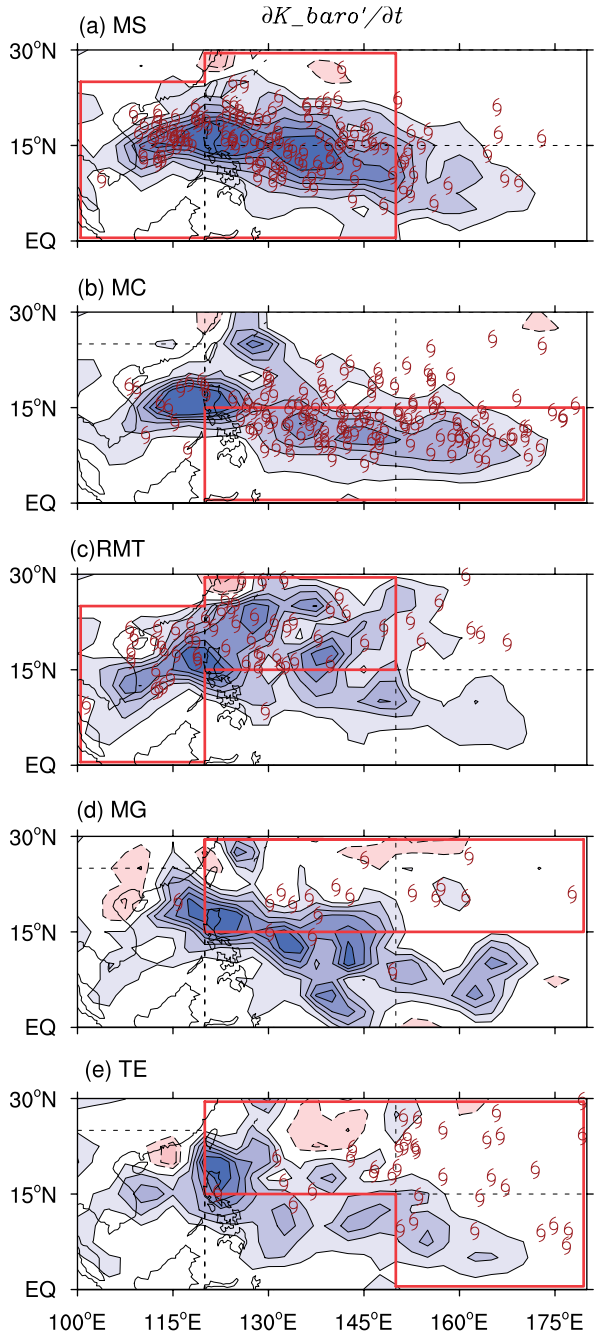

Figure 8. The composite horizontal distributions of the time change rate of EKE at 850 hPa due to the barotropic energy conversion in various large-scale circulation pattern during 1991–2010. Unit: $10^{-6}\mathrm{m}^2\,\mathrm{s}^{-3}$, contour interval is 8. The solid and dashed lines indicate positive and negative values, and the values over 8 or below −8 are shaded. (a) MS pattern; (b) MC pattern; (c) RMT pattern; (d) MG pattern; (e) TE pattern.

Here, we only examine the contribution of each term in the right side of Equation ((1) to the increase of EKE in the MS, MC, and RMT patterns.

For those TCs in the MS pattern, the kinetic energy conversion is dominated by the term $-\overline{u'v'}\partial\overline{u}/\partial y$ in NW and SW parts of the WNP (Figure 9(a)). Thus, cyclonic shear of the basic flow over these regions is of a key importance in the increase of EKE. The

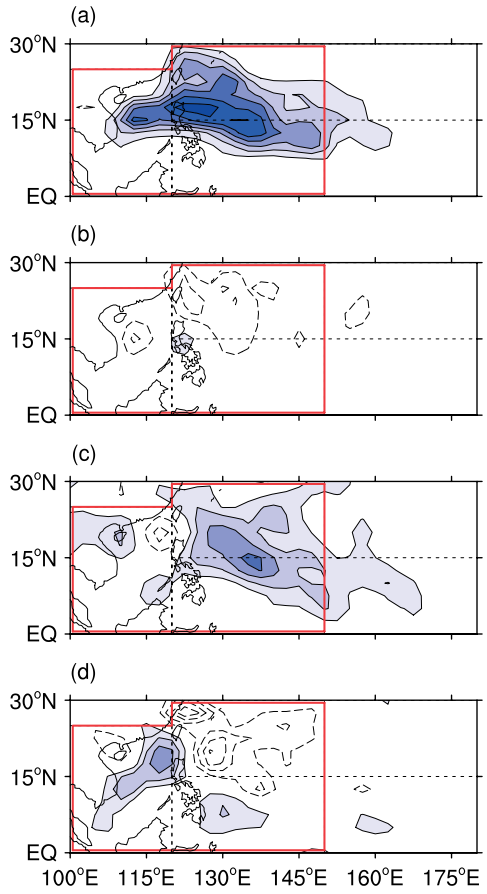

Figure 9. The horizontal distribution of each term on the right-hand-side of Equation ((1) of the 850 hPa EKE time change rate due to the barotropic energy conversion for the MS pattern (unit: $10^{-6}\mathrm{m}^2\,\mathrm{s}^{-3}$), contour interval is 8. The solid and dashed lines indicate positive and negative values, and the values over 8 are shaded. (a) Meridional shear of zonal wind term $-\overline{u'v'}\partial\overline{u}/\partial y$. (b) Zonal shear of meridional wind term $-\overline{u'v'}\partial\overline{v}/\partial x$. (c) Zonal wind convergence term $-\overline{u'^2}\partial\overline{u}/\partial x$. (d) Meridional wind convergence term $-\overline{v'^2}\partial v/\partial y$.

third term $-\overline{u'^2}\partial\overline{u}/\partial x$ also plays an important role for the increase of EKE in the western part of the WNP (Figure 9(c)). This indicates that the barotropic wave energy accumulates in this region due to the zonal wind convergence, consistent with previous studies (Webster and Chang, 1988; Hartmann and Maloney, 2001). Over the SCS, the contribution of meridional convergence of meridional wind, i.e. $-\overline{v'^2}\partial\overline{v}/\partial y$ could not be neglected (Figure 9(d)). The second term in the right-hand-side of Equation (1) is negative and its value is relatively small compared to the other three terms (Figure 9(b)).

For TCs that form in the MC pattern, the first term $-\overline{u'v'}\partial\overline{u}/\partial y$ and the third term $-\overline{u'^2}\partial\overline{u}/\partial x$ play comparable roles in SE and SW parts of the WNP (Figure 10(a) and (c)). The term $-\overline{u'v'}\partial\overline{u}/\partial y$ is smaller compared to that in the MS pattern, which may be attributed to the weak meridional shear of zonal wind. The contribution of zonal shear of meridional wind and convergence is relatively small for the TC formation in the MC pattern (Figure 10(b) and (d)).

© 2013 Royal Meteorological Society

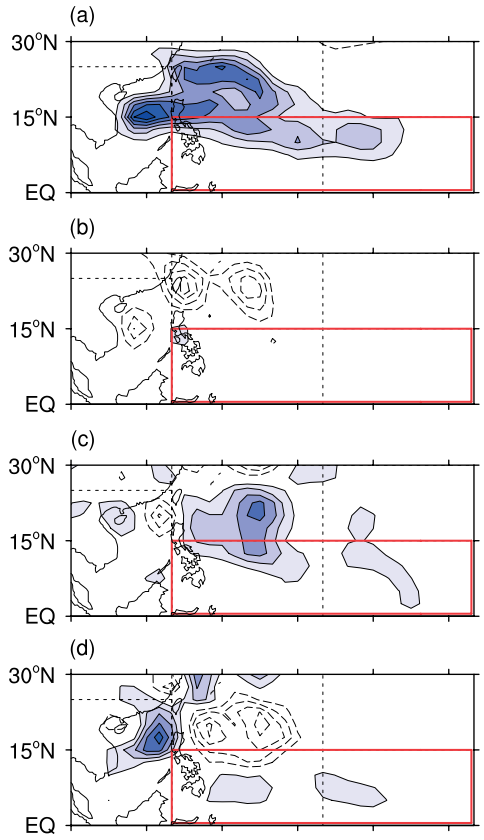

Figure 10. The horizontal distribution of each term on the right-hand-side of Equation ((1) of the 850 hPa EKE time change rate due to the barotropic energy conversion for the MC pattern (unit: $10^{-6}\mathrm{m}^2\,\mathrm{s}^{-3}$), contour interval is 8. The solid and dashed lines indicate positive and negative values, and the values over 8 are shaded. (a) Meridional shear of zonal wind term $-\overline{u'v'}\partial\overline{u}/\partial y$. (b) Zonal shear of meridional wind term $-\overline{u'v'}\partial\overline{v}/\partial x$. (c) Zonal wind convergence term $-\overline{u'^2}\partial\overline{u}/\partial x$. (d) Meridional wind convergence term $-\overline{v'^2}\partial v/\partial y$.

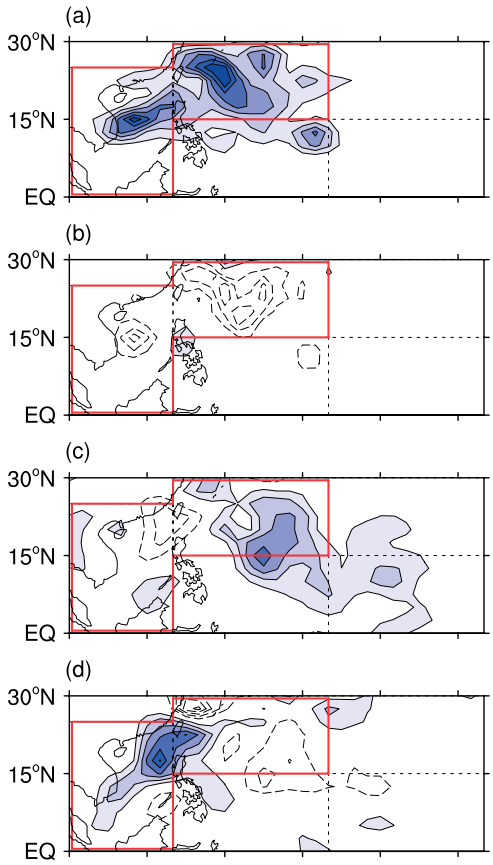

Figure 11. The horizontal distribution of each term on the right-hand-side of Equation ((1) of the 850 hPa EKE time change rate due to the barotropic energy conversion for the RMT pattern (unit: $10^{-6}\mathrm{m}^2\,\mathrm{s}^{-3}$), contour interval is 8. The solid and dashed lines indicate positive and negative values, and the values over 8 are shaded. (a) Meridional shear of zonal wind term $-\overline{u'v'}\partial\overline{u}/\partial y$. (b) Zonal shear of meridional wind term $-\overline{u'v'}\partial\overline{v}/\partial x$. (c) Zonal wind convergence term $-\overline{u'^2}\partial\overline{u}/\partial x$. (d) Meridional wind convergence term $-\overline{v'^2}\partial v/\partial y$.

When TCs form in the RMT circulation, the term of meridional shear of zonal wind $-\overline{u'v'}\partial\overline{u}/\partial y$ contributes to the barotropic kinetic energy conversion in the SCS and NW quadrant of the WNP, along the trough axis (Figure 11(a)). The terms of $-\overline{u'^2}\partial\overline{u}/\partial x$ and $-\overline{v'^2}\partial\overline{v}/\partial y$ have a large contribution to the increase of EKE in the NW part of the WNP and the SCS, respectively (Figure 11(c) and (d)). The contribution of $-\overline{u'v'}\partial\overline{u}/\partial y$ term is comparable to the sum of the latter two terms. The zonal shear of the meridional wind appears to have a negative contribution (Figure 11(b)).

In theory, the necessary condition for EKE growth is that the atmospheric is barotropically unstable, which represents that there is Maximum or minimum absolute vorticity in the flow fields. So we examined the absolute vorticity gradient, and it is found that the potential zeros of the absolute vorticity gradient spreads along the axis of the monsoon trough. That is to say, the maximum absolute vorticity lies nearby the axis of the monsoon trough. Inside the monsoon trough, the atmospheric is always barotropically unstable, which is favourable for the EKE growth.

From the above results, the meridional shear of zonal wind has a leading contribution to the barotropic energy conversion in the WNP region, followed by the zonal convergence of zonal wind. In the SCS region, the meridional wind convergence has an important contribution to the increase of the EKE. The shear of meridional wind has a weak and negative role.

5. Conclusions and discussions

This study analysed the large-scale patterns favourable to tropical cyclogenesis over the WNP in typhoon seasons for the period 1991–2010. Five circulation patterns are classified based on low-level wind distribution in the preformation period. These patterns are MS, MC, MG, RMT, and TE. Among them, MS and MC are two major patterns, accounting for 33.1% and 33.2% of all TC genesis cases in the analysis period. The RMT pattern accounts for 15.1% of the TC genesis cases. Only 4.2% and 8.7% of TCs form in the MG and TE patterns, respectively. The monsoon-related tropical cyclogenesis

© 2013 Royal Meteorological Society

cases occupy 85.4% of total events during the WNP typhoon season from July to October.

Composite analysis shows that tropical cyclogenesis over the WNP is highly modulated by 200 hPa divergence, OLR, VWS, 700–500 hPa relative humidity, and 850 hPa relative vorticity. While the MS, MC, and RMT patterns provide favourable low-level vorticity, high-level divergence, small VWS, mid-tropospheric humidity, and convective activity for TC genesis, not all the above conditions are in favour of the TC genesis in the MG and TE patterns. For example, the high-level divergence is not favourable in the MG pattern. In the TE pattern, the mid-tropospheric relative humidity and low-level relative vorticity appear not to be in a favourable condition for the TC genesis.

The analysis of barotropic energy conversion indicates that it may be the main mechanism for the EKE growth in the MS, MC, and RMT patterns. In the MS pattern, $-\overline{u'v'}\partial\overline{u}/\partial y$ is the leading source of energy conversion from mean flow to eddy. In the MC pattern, the meridional shear of zonal wind term $-\overline{u'v'}\partial\overline{u}/\partial y$, zonal convergence term $-\overline{u'^2}\partial\overline{u}/\partial x$, and the meridional convergence term $-\overline{v'^2}\partial\overline{v}/\partial y$ all play important roles in the increase of the EKE. In the RMT pattern, the term $-\overline{u'v'}\partial\overline{u}/\partial y$ makes a large contribution to the growth of the EKE in both the SCS and NW quadrant of the WNP, and comparable effects come from terms $-\overline{u'^2}\partial\overline{u}/\partial x$ over the WNP and $-\overline{v'^2}\partial\overline{v}/\partial y$ over the SCS. In the MG and TE patterns, the region of barotropic energy conversion is not consistent with the region of TC genesis, indicating the role of other energy sources.

For the TCs in the MG pattern, some detailed analysis indicates that when a MG circulation establishes, the low-level vorticity displays several centres inside the gyre, which is unfavourable for a concentrated conversion of mean kinetic energy to EKE. Thus, the large-scale circulation cannot provide kinetic energy to tropical cyclogenesis in this pattern. The MG pattern features higher mid-level humidity and active convection as discussed above. The deep convection and development of vortical hot towers enhance diabatic heating. Moreover, we have examined all cases in the MG pattern using infrared satellite images (not shown) and the merging processes of mesoscale convective systems (MCS) appear in most events. The diabatic heating and the merging of convective systems can tremendously strengthen the low-level vorticity, and thus may lead to a TC formation. The role of MCSs for tropical cyclogenesis is confirmed by both statistical studies (Ritchie and Holland, 1999; Lee *et al.*, 2008) and case studies (Houze *et al.*, 2009; Hogsett and Zhang, 2010). Nevertheless, the MG provides an important environment for the TC genesis in this category.

For TCs genesis in the TE pattern, we have applied a composite diagnosis similar to Ritchie and Holland (1999). The obtained result is similar to that by Ritchie and Holland (1999). For example, when an easterly wave-like disturbance with maximum amplitude at 700-hPa shifts westward, it causes the development of TCs. Some high-resolution dataset should be adopted to investigate the physical mechanism for TC genesis in the easterlies over the WNP.

In this study, we did not investigate the linkage between the patterns and TCs genesis frequency. For example, the MG pattern rarely appears over the WNP, but a series of TCs may form inside the gyre when the MG pattern is established (Lander 1994). It implied that the MG pattern may be as favourable to tropical cyclogenesis as the MS and MC patterns. How are the 'favourabilities' for tropical cyclogenesis of these large-scale patterns? This question should be addressed in future.

Acknowledgements

This study was reported on the 30th Conference on Hurricanes and Tropical Meteorology held at Florida USA during 14–20 April 2012 and the Cross-strait Joint Symposium on Typhoon Activity over the western North Pacific held at Zhang-Jia-Jie city, Hunan province, China during 26–30 April 2012. The authors are grateful to Dr. Renguang Wu from the Chinese University of Hong Kong for constructive comments and helpful modification for our manuscript. We also thank Prof. Tim Li from the University of Hawaii and Dr David S. Nolan from the University of Miami and two reviewers for their useful suggestions. This study was supported by the Special Scientific Research project for Public Interest (Grant No. GYHY201006021 and GYHY200806009), the National Natural Science Foundation of China (Grant No. 41275001, 40921160379 and 41075039).

References

Briegel LM, Frank WM. 1997. Large-scale influences on tropical cyclogenesis in the western North Pacific. *Monthly Weather Review* **125**: 1397–1413.

Chang L-Y, Cheung KKW, Lee C-S. 2010. The role of trade wind surges in tropical cyclone formations in the western North Pacific. *Monthly Weather Review* **138**: 4120–4134.

Chen G. 2009. Interdecadal variation of tropical cyclone activity in association with summer monsoon, sea surface temperature over the western North Pacific. *Chinese Science Bulletin* **54**: 1417–1421.

Chen G, Huang R. 2008. Influence of monsoon over the warm pool on interannual variation on tropical cyclone activity over the western North Pacific. *Advances Atmospheric Sciences* **25**: 319–328.

Chen G, Sui C-H. 2010. Characteristics and origin of quasi-biweekly oscillation over the western North Pacific during boreal summer. *Journal of Geophysical Research-Atmospheres* **115**: D14113.

Chen T-C, Wang S-Y, Yen M-C, Gallus WA. 2004. Role of the monsoon gyre in the interannual variation of tropical cyclone formation over the western North Pacific. *Weather and Forecasting* **19**: 776–785.

Cheung KKW. 2004. Large-scale environmental parameters associated with tropical cyclone formations in the western North Pacific. *Journal of Climate* **17**: 466–484.

Chia HH, Ropelewski CF. 2002. The interannual variability in the genesis location of tropical cyclones in the Northwest Pacific. *Journal of Climate* **15**: 2934–2944.

Ferreira RN, Schubert WH. 1997. Barotropic aspects of ITCZ breakdown. *Journal of the Atmospheric Sciences* **54**: 261–285.

Frank WM, Roundy PE. 2006. The role of tropical waves in tropical cyclogenesis. *Monthly Weather Review* **134**: 2397–2417.

© 2013 Royal Meteorological Society

Fu B, Li T, Peng MS, Weng F. 2007. Analysis of tropical cyclogenesis in the western North Pacific for 2000 and 2001. *Weather and Forecasting* **22**: 763–780.

Georgiadis AP, Bigg G. 2007. Environmental links to reduced tropical cyclogenesis over the south-east Caribbean. *International Journal of Climatology* **27**: 989–1001.

Goh AZ-C, Chan JCL. 2010. Interannual and interdecadal variations of tropical cyclone activity in the South China Sea. *International Journal of Climatology* **30**: 827–843.

Gray WM. 1968. Global view of the origin of tropical disturbances and storms. *Monthly Weather Review* **96**: 669–700.

Gray WM. 1998. The formation of tropical cyclones. *Meteorology and Atmospheric Physics* **67**: 37–69.

Harr PA, Elsberry RL. 1995. Large-scale circulation variability over the tropical western North Pacific. Part I: Spatial patterns and tropical cyclone characteristics. *Monthly Weather Review* **123**: 1225–1246.

Hartmann DL, Maloney ED. 2001. The Madden–Julian oscillation, barotropic dynamics, and North Pacific tropical cyclone formation. Part II: Stochastic barotropic modeling. *Journal of the Atmospheric Sciences* **58**: 2559–2570.

Hogsett W, Zhang D-L. 2010. Genesis of typhoon Chanchu (2006) from a westerly wind burst associated with the MJO. Part I: Evolution of a vertically tilted precursor vortex. *Journal of the Atmospheric Sciences* **67**: 3774–3792.

Houze RA, Lee W-C, Bell MM. 2009. Convective contribution to the genesis of hurricane Ophelia (2005). *Monthly Weather Review* **137**: 2778–2800.

Kanamitsu M, Ebisuzaki W, Woollen J, Yang S-K, Hnilo JJ, Fiorino M, Potter GL. 2002. NCEP-DOE AMIP-II Reanalysis (R-2). *Bulletin of the American Meteorological Society* **83**: 1631–1643.

Krouse KD, Sobel AH. 2010. An observational study of multiple tropical cyclone events in the western north Pacific. *Tellus A* **62**: 256–265.

Lander MA. 1994. Description of a monsoon gyre and its effects on the tropical cyclones in the western North Pacific during August 1991. *Weather and Forecasting* **9**: 640–654.

Lander MA. 1996. Specific tropical cyclone track types and unusual tropical cyclone motions associated with a reverse-oriented monsoon trough in the western North Pacific. *Weather and Forecasting* **11**: 170–186.

Lee C-S, Lin Y-L, Cheung KKW. 2006. Tropical cyclone formations in the South China Sea associated with the Mei-Yu front. *Monthly Weather Review* **134**: 2670–2687.

Lee C-S, Cheung KKW, Hui JSN, Elsberry RL. 2008. Mesoscale features associated with tropical cyclone formations in the western North Pacific. *Monthly Weather Review* **136**: 2006–2022.

Li T, Fu B. 2006. Tropical cyclogenesis associated with Rossby wave energy dispersion of a preexisting typhoon. Part I: Satellite data analyses. *Journal of the Atmospheric Sciences* **63**: 1377–1389.

Maloney ED, Hartmann DL. 2001. The Madden–Julian oscillation, barotropic dynamics, and North Pacific tropical cyclone formation. Part I: Observations. *Journal of the Atmospheric Sciences* **58**: 2545–2558.

P-c H, Li T, Tsou C-H. 2010. Interactions between boreal summer intraseasonal oscillations and synoptic-scale disturbances over the western North Pacific. *Part I: Energetics Diagnosis. Journal of Climate* **24**: 927–941.

Ritchie EA, Holland GJ. 1999. Large-scale patterns associated with tropical cyclogenesis in the Western Pacific. *Monthly Weather Review* **127**: 2027–2043.

Schreck CJ, Molinari J. 2009. A case study of an outbreak of twin tropical cyclones. *Monthly Weather Review* **137**: 863–875.

Sobel AH, Bretherton CS. 1999. Development of synoptic-scale disturbances over the summertime tropical Northwest Pacific. *Journal of the Atmospheric Sciences* **56**: 3106–3127.

Ventham JD, Wang B. 2007. Large-scale flow patterns and their influence on the intensification rates of western North Pacific tropical storms. *Monthly Weather Review* **135**: 1110–1127.

Webster PJ, Chang H-R. 1988. Equatorial energy accumulation and emanation regions: impacts of a Zonally varying basic state. *Journal of the Atmospheric Sciences* **45**: 803–829.

Wu L, Wen Z, Huang R, Wu R. 2011. Possible linkage between the monsoon trough variability and the tropical cyclone activity over the western North Pacific. *Monthly Weather Review* **140**: 140–150.

Yoshida R, and Ishikawa H. 2013. Environmental factors contributing to tropical cyclone genesis over the western North Pacific. *Monthly Weather Review* **141**: 451–467.

© 2013 Royal Meteorological Society